# Influence of the opening angle between two sprays in diverging nozzles

V. Luckhchoura*, R. Pardeshi[1], A. Sharma[1], S. Vogel[1], N. Peters[1],
M. Cárdenas[2] and R. Kneer[2]
1 Institut für Technische Verbrennung
2 Institut für Wärme- und Stoffübertragung
RWTH Aachen University

**Abstract**

In the cluster nozzle concept, each orifice of a conventional nozzle is replaced by two smaller orifices yielding the same flow rate. The opening angle between two sprays was positive, thus the nozzles were called diverging. In this study, numerical simulations of three cluster nozzles were performed in a chamber at 800 K ambient temperature and 50 bar ambient pressure conditions. First, the computed liquid and vapor penetration lengths were compared with the measured penetrations to validate the model. Then, the computed results were further analyzed to examine the influence of spray-spray interaction due to varying opening angle between the sprays on droplet breakup, spray shape and evaporation leading to mixture preparation.

## Introduction

The reduction of the orifice diameter in nozzles for diesel injectors enhances the mixing processes in the spray and leads to leaner equivalence ratios, which are known to reduce soot formation [1]. Therefore, nozzles with more and smaller orifices have contributed significantly to the improvement of diesel engines in the past years. However, above a certain number of orifices, no further improvement is recorded for equispaced orifice configurations [2, 3]. The reason for this is probably an increased interaction between the sprays for an increased number of orifices per nozzle. There are several possibilities to enhance engine performance by the usage of more sprays per nozzle. One possibility is to cluster/group the orifices [4, 5]. For this purpose each orifice of a conventional nozzle is replaced by two smaller orifices, which are sized to yield the same flow rate. The basic strategy of the cluster configuration is to enhance droplet breakup, and therefore a better mixture formation, caused by the smaller nozzle orifices with a comparable penetration length of the vapor phase to the penetration length of the conventional configuration due to the merging of the spray plumes. Many possible improvements have been reported for diverging nozzles. Diverging nozzles are also called as group-hole/cluster nozzles. Gao et al. [5] conducted an experimental study on spray and mixture properties of the group-hole nozzle by means of the ultraviolet-visible laser absorption-scattering (LAS). In this study comparative analysis of a group-hole nozzle and a single-hole nozzle was done. The orifice diameter of the group-hole was 0.095 mm, maintaining the same total cross-sectional area as that of the single-hole nozzle. The two orifices of the group-hole nozzle were parallel and the interval between them was 0.204 mm. Experiments were carried out for non-evaporating and evaporating conditions [5]. Under evaporative conditions the maximum value of equivalence ratio for the vapor phase was increased and vapor/gas mixture, with relatively high equivalence ratios, was wider dispersed by the group-hole nozzle. Thus group-hole nozzle had positive effect in enhancing fuel evaporation and consequently fuel and air mixing to some extent. Mixture properties, including the mass of entrained gas, vapor fuel, evaporation ratio, can be improved using the group-hole nozzle, this was more evident at a high injection pressure, i.e. at 1200 bar. This was helpful for forming a leaner, more homogeneous fuel and gas mixture. Under non-evaporating conditions spray shape of the group-hole nozzle, was very similar to the single-hole nozzle. However, there was a slight decrease in spray-tip penetration and spray angle. The smaller Sauter Mean Diameter (SMD) can be achieved using the group-hole nozzle, indicating that the group-hole has the potential to improve fuel atomization. It was expected that nozzle specifications greatly impacts on spray behavior and mixture properties and should be optimized to promote the benefits of group-hole nozzle.

Nishida et al. [6] experimentally investigated the effects of a group-hole nozzle specifications on spray and mixture properties by varying the opening angle and the spacing between orifices. Opening angle between orifices was varied from 0° up to 10°. Group-hole nozzle arrangements with various intervals (0.1, 0.287, 0.687 mm) were selected and compared to the single-hole nozzle. It was observed that with the increase in the opening angle between orifices, spray penetration becomes shorter and spray disperses more widely. On other side, the liquid phase region is observed around the spray tip for the divergent group-hole nozzles and the amount of liquid fuel

*Corresponding author: vluckhchoura@itv.rwth-aachen.de

is higher than that of the single-hole nozzle, which is primarily due to the droplets collision and coalescence in the overlapping part of the two sprays. Increasing the opening angle, the two sprays appeared to be separated to some extent, thus resulting in less droplet collision between the sprays. The high amount of liquid fuel can therfore be avoided, corresponding significant increase in mass of vapor fuel. This indicated an evaporation improvement. An increase in the spacing decreases the effect of the direct collision between two sprays, whereas more droplets collision and coalescence supposedly occur within the spray due to the decreased tip penetration. It was found that the larger the spacing between the orifices is, the more liquid fuel remains within the spray. From the viewpoint of better fuel atomization and evaporation characteristics, the diverging opening angle between orifices is more effective parameter than the spacing between the parallel orifices (0° included angle).

Suh et al. [7] investigated the influence of a group-hole nozzle on the atomization characteristics of a biodiesel fuel. Experiments were carried out at injection pressure of 800 bar and ambient pressure of 1 bar. The single-hole nozzle consisted eight holes each with diameter of 0.128 mm. The group-hole nozzle had two groups of eight holes with a diameter 0.09 mm and separated by a distance of 0.2 mm. The diverging opening angle between two holes in the group-hole nozzle was 22.5°. SMD distribution from the group-hole nozzle has a larger droplet diameters compared to the single-hole nozzle. This is due to collision and coalescence of droplets, leading to the increase in droplet diameters.

In this study, influence of diverging opening angle between the two orifices is investigated in a pressurized vessel under thermodynamic conditions relevant for diesel engines. For the macroscopic behavior of the sprays, experimental visualization techniques were employed. A de-focused laser light sheet was used to detect the liquid phase of the spray. The vapor phase was detected with a simple Schlieren technique. Corresponding numerical simulations provided additional insight on spray characteristics like spray shape, droplet sizes and evaporation due to interaction of diverging sprays.

## Materials and Methods

### *Experimental setup and Measurement techniques*

Cárdenas et al. [8] presented a detailed experimental investigation of cluster nozzles through quasi simultaneous measurement of several spray quantities. Within the experimental study, six cluster nozzles with varying opening angle from 0° up to 15° and two conventional nozzles were investigated. All cluster nozzles had the identical flow rate of 210 $cm^3$/30s. Two conventional nozzles having flow rates of 210 and 105 $cm^3$/30s were used as reference nozzles. Cluster nozzles had 6 orifices distributed in 3 groups as shown in Fig. 1.

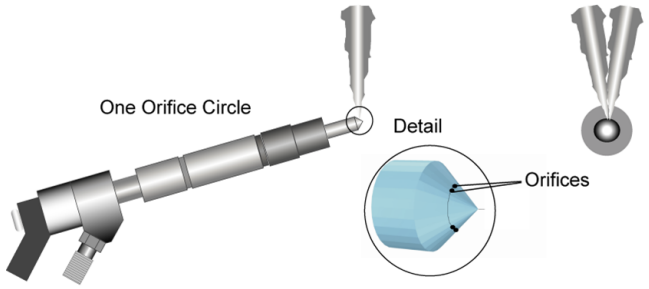


**Figure 1.** Sketch of the orifice orientation for the investigated diverging cluster nozzles

The common rail injector was installed in a pressurized vessel and experiments were conducted in a nearly quiescent high-pressure (50 bar) and high temperature (800 K) conditions. Nozzles were investigated at three injection pressures of 600 bar, 1100 bar and 1600 bar and an energizing time of 850 $\mu$s. Nozzles were installed on a state-of-the-art Bosch piezo injector. The fuel used for this experimental study was diesel according to the European Standard EN 590. The liquid and vapor phases were visualized using scattered light of Nd:YAG laser and back-lit schlieren imaging, respectively. The penetration lengths of the liquid and the vapor phase were determined and analyzed. From the analysis of the results, cluster nozzles with same behavior were grouped together. They were grouped as conventional nozzle behavior, transition behavior and low interaction behavior.

### *Numerical Methods*

For simulations, one opening angle representing each group was selected, i.e. 0°, 7.5° and 15°. The simulations were performed at a injection pressure of 1600 bar and an energizing time of 850 $\mu$s. CFD code used is AC-Flux (formerly known as GMTEC). It is a flow solver based on finite volume methods that employs unstructured, mostly

hexahedral meshes. AC-Flux solves partial differential equations for the Navier-Stokes equations, one equation for total enthalpy and two equations to account for the turbulence, i.e. standard $k$-$\varepsilon$ model. In addition, two equations for the mean mixture fraction and its variance describing mixing field are also solved. AC-FluX has been documented in detail by Ewald et al. [9].

The liquid phase is modeled using the discrete droplet model (DDM). Since the spray consists of a large number of droplets, only the behavior of a representative subset of all droplets (called parcels) is calculated in detail. Each parcel represents an ensemble of droplets. Within one parcel, all droplets have same properties. The ensemble of all parcels provides the statistical information on the spray. All the subprocesses that are not resolved on the parcel level are modeled using a Monte-Carlo method. The gas phase and the liquid phase are coupled through source terms in the governing equations for the gas phase. Mass, momentum and energy are exchanged between the discrete parcels and the appropriate underlying cell. Furthermore, the $k$-$\varepsilon$ equations contain source terms describing the effect of turbulent dispersion of droplets on the turbulent kinetic energy and dissipation of the turbulent kinetic energy, respectively. These source terms are also evaluated on the appropriate underlying cells. The DDM approach is therefore also referred to as a Lagrangian-Eulerian approach. An advantage of the DDM approach is that the nozzle-hole diameter does not need to be resolved by the computational mesh.

Spray submodels were used for each of the spray subprocesses like breakup, collision, coalescence, evaporation and dispersion. Droplet breakup of a liquid jet in gaseous fluid occurs due to instabilities induced by velocity and density gradients across the interface between liquid and gaseous phase, known as Kelvin-Helmholtz and Reyleigh-Taylor instabilities respectively. Two droplet regimes exist: primary and secondary breakup. In this work, primary breakup is not considered. All parcels are initialized by the same initial SMD and not by monodisperse distribution function with size distribution around SMD. The secondary breakup was modeled by Kelvin-Helmholtz (KH) and Reyleigh-Taylor (RT) models. For modeling droplet collision, only parcels approaching each other are considered in parcel-parcel interaction. Also, the parcels have to reside in a sphere spanned by given collision radius in order to be considered for parcel-parcel interaction. Because, the collision probability function is inversely proportional to the considered volume, a larger collision radius and, therefore a higher collision frequency will not necessarily lead to a larger collision probability. For modeling droplet evaporation, droplets are assumed spherical with uniform temperature, and radiative heat transfer was neglected. A detailed description of the spray modeling in AC-FluX can be found in Spiekermann et al. [10]. A major aspect in modeling diesel engine combustion is the treatment of chemistry. The surrogate fuel (IDEA) for diesel used in this work is a mixture of 70 percent n-decane and 30 percent $\alpha$-methylnaphthalene by liquid volume. The complete chemical reaction mechanism comprised 506 elementary reactions and 118 chemical species. Further details can be obtained from [11]. Injection rate was taken from rate measurements using a the Bosch type flow bench.

**Results and Discussion**

In the CFD simulations, the spray chamber was represented by a cylinder that was meshed by means of an O-grid topology. The finest mesh resolution was in the area around the nozzle, with a cell size of approximately 1.0 mm in each direction as shown in Fig. 2. The radius of the computational domain was 50.0 mm and the height was 90.0 mm.

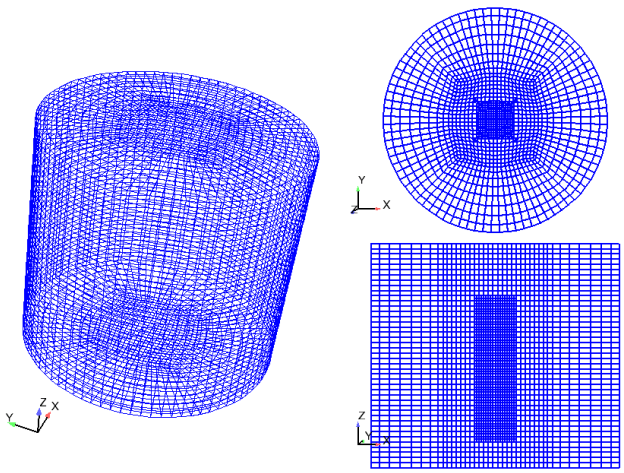


**Figure 2.** Computational mesh for the investigated spray chamber

Three cluster nozzles, with opening angle of 0°, 7.5° and 15° respectively, were simulated at 1600 bar rail pressure and an energizing time of 850 $\mu$s, as mentioned in the previous section. The actual duration of injection was 1.0 ms as shown in Fig. 3. The figure shows a measured injection rate, which is same for all the nozzles.

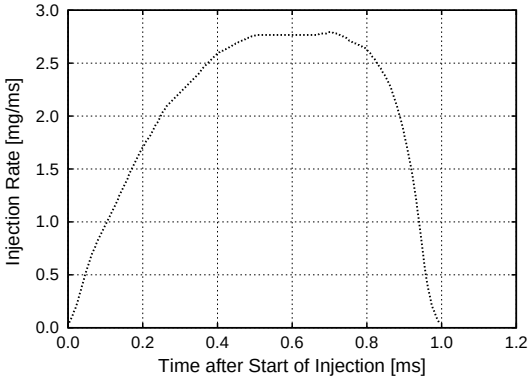


**Figure 3.** Measured injection rate for all the nozzles

Penetration lengths of the liquid and the vapor phase obtained from simulations are in good agreement with experimental data for all three diverging cluster-nozzles, as it can be seen in Fig. 4. Similar to the experiments, penetration length of both phases in the simulations shows strong dependence on the opening angle between two sprays of the cluster-nozzles. Up to 0.4 ms after start of injection, liquid and gas penetration were very similar for all the opening angles. After that liquid and gas penetration started to differ. With increasing opening angle, the liquid and the vapor penetration length decreased for the diverging nozzles, i.e. the diverging nozzle with 0° opening angle has the highest and with 15° opening angle has the lowest liquid and vapor penetration lengths as shown in Fig. 4(a), 4(b) and 4(c). This suggests that lowering the opening angle leads to faster axial pentration of both liquid and vapor sprays in the vessel.

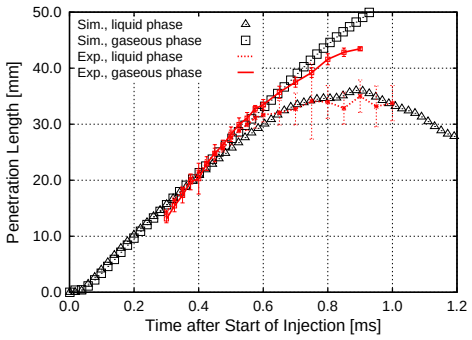


(a) 0° opening angle

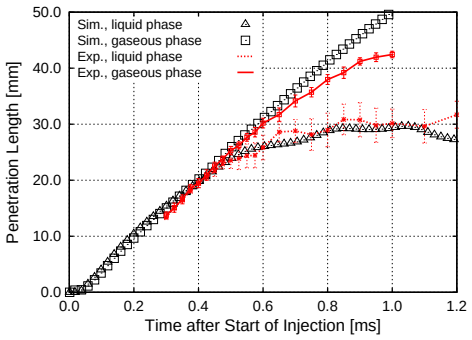


(b) 7.5° opening angle

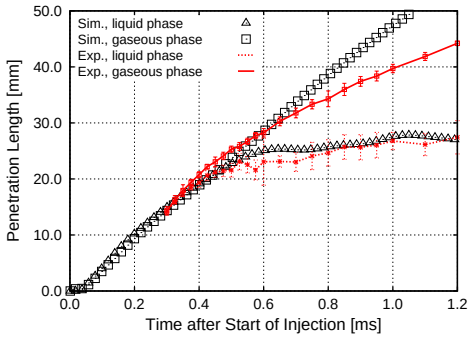


(c) 15° opening angle

**Figure 4.** Spray penetration comparison for varying opening angle

For the sake of clarity, figures 5(a) and 5(b) show the computed liquid and gas penetration length over time. It can be observed that liquid penetration reached its maximum value earlier with increasing opening angle. After reaching the maximum value, liquid penetration decreased slightly for 0° opening angle. In case of 15° opening angle, liquid penetration remained constant after reaching its maximum value. While gas penetration went on increasing continuously with time for all the opening angles. Higher liquid penetration for lower opening angle can be verified from droplet size distribution.

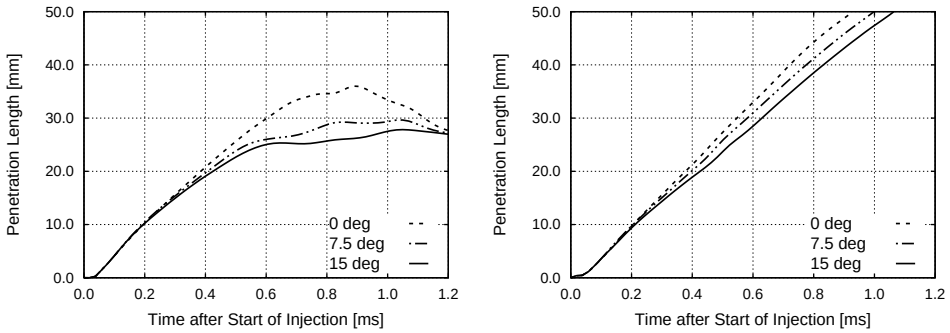


(a) Liquid Penetration (b) Vapor Penetration

**Figure 5.** Liquid and vapor penetration comparison for varying opening angle

Figure 6 shows droplet size distribution for all the three cluster nozzles at 0.6 ms after start of injection. As seen in the figure, with the increase in the opening angle the separation between the sprays increased. As a result of completely merged sprays for the cluster nozzle with 0° angle, droplet collision between the sprays increased, which resulted in the larger droplet sizes. The larger the droplet size is, the higher is the penetration. Thus, nozzle with 0° angle penetrated deepest in the vessel compared to other diverging cluster nozzles. At 15° opening angle, the sprays were almost separated resulting in lower droplet coalescence and thus, droplet breakup within the spray was the dominant process forming smaller-sized droplets as seen in Fig. 6.

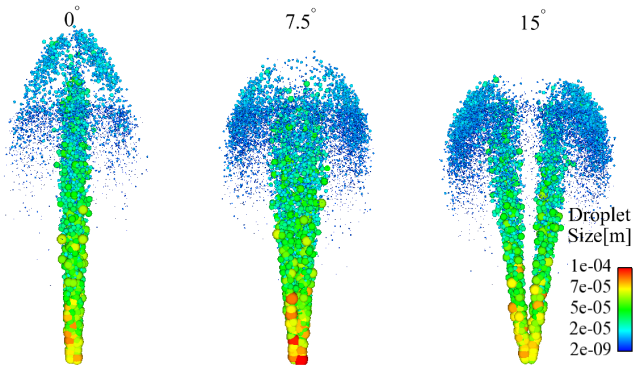


**Figure 6.** Spray shape comparison for varying opening angle at 0.6 ms after start of injection: front view

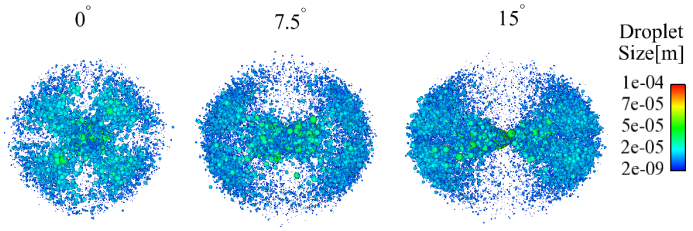


**Figure 7.** Spray shape comparison for varying opening angle at 0.6 ms after start of injection: top view

Accordingly, atomization was better and the spray penetration was lower. Spray shape also differed with varying opening angle. Spray tip shape for 0° opening angle was cone shaped, while for 15° opening angle it was mushroom shaped. Overall spray shape for 15° opening angle was found to be wider than in case of 0°. Cluster opening angle of 7.5° had intermediate results. Spray shape as viewed from top also differed considerably (see Fig. 7). For 0° opening angle, droplets were distributed equally around the sprays giving spherical shape structure. But, for higher opening angle droplets were distributed more non-uniformly. Thus, for 15° opening angle droplets are spread only on two sides of spray therefore forming ellipsoid shape.

Next, axial velocity for three opening angles are compared. At 0.7 ms after start of injection, axial velocities were analyzed at two axial distances: at 25 mm (Fig. 8(a)) and at 35 mm (Fig. 8(b)) away from the nozzle exit in the axial direction of sprays. Both figures show that for 0° opening angle, axial velocity is the highest at the centerline of spray and 15° opening angle resulted in the lowest axial velocity at the centerline of spray. Opening angle of 7.5° resulted in the intermediate axial velocity. Difference between centerline axial velocities widens at higher axial distance from the nozzle exit as seen in Fig. 8(b). Axial velocity away from the centerline show different trends in both figures for all the three opening angles. In Fig. 8(a) lower centerline velocity for higher opening angles is offset by higher axial velocity away from the centerline. Whereas at 35 mm (Fig. 8(b)) lowering the opening angle not only results into higher centerline axial velocity but also higher velocity in the radial direction. Thus, opening angle variation has a considerable effect on axial velocity of gas which affect spray penetration. It was also observed that the axial velocity distribution for all the opening angles had negative axial velocity near to both sides of spray, thus showing flow in the opposite direction of sprays.

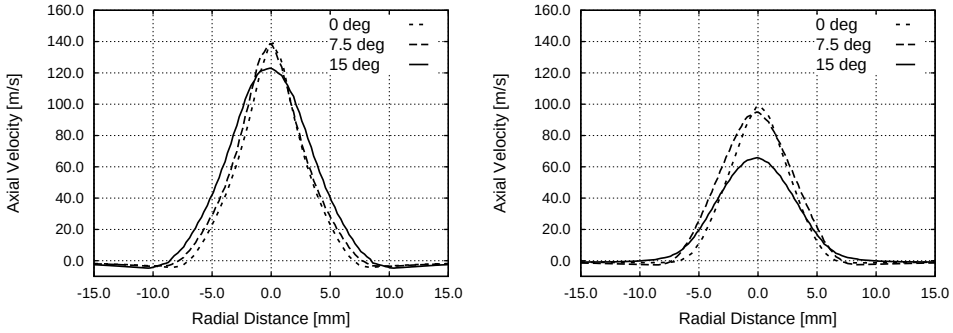


(a) 25 mm away from the nozzle exit (b) 35 mm away from the nozzle exit

**Figure 8.** Axial velocity variation at two axial distances from the nozzle exit at 0.7 ms after start of injection

To examine the spray evaporation characteristics of the diverging cluster nozzles, evaporation rate and Sauter Mean Radius (SMR) over time are shown for each nozzle in Figs. 9(a) and 9(b) respectively. Both figures are aimed to demonstrate the interrelation between evaporation rate and SMR. In Fig. 9(b), a decrease in SMR could be due to droplet breakup or due to fuel evaporation. Whereas an increase in SMR could be a result of droplet collision and coalescence, decrease in injection rate near the end of injection or simply the result of statistics in the wake of smaller droplets being evaporated such that only the larger droplets remain in the computational domain. Initially up to 0.5 ms (in Fig. 9(a)), evaporation rate is the highest for 15° opening angle and the lowest for 0° opening angle. For the corresponding duration, SMR is the highest for 0° and all the nozzles show a continuous reduction in SMR. One may anticipate that droplet breakup and fuel evaporation processes were occurring at the same time thus causing a continuous reduction in the SMR for all the nozzles. In the next 0.1 ms, evaporation rate for 0° and 7.5° became higher than for 15°. Accordingly, the SMR evolution showed a rather faster decay for 0° and 7.5° opening angles. Shortly after 0.6 ms the SMR for 0° and 7.5° opening angles started to increase, resulting in lower evaporation rates compared to the 15° opening angle. This increase in the SMR could be due to one of the reasons mentioned in the beginning of this paragraph. Since the injection rate is constant (Fig. 3) and the evaporation rate is decreasing, the only most probable reason is the droplet collision and coalescence between the sprays for 0° and 15° opening angles. After 0.9 ms, a monotonic increase of the SMR for all the nozzles could be a result of droplets being injected near the end of injection, and remaining of larger droplets due to evaporation of smaller droplets in the computational domain.

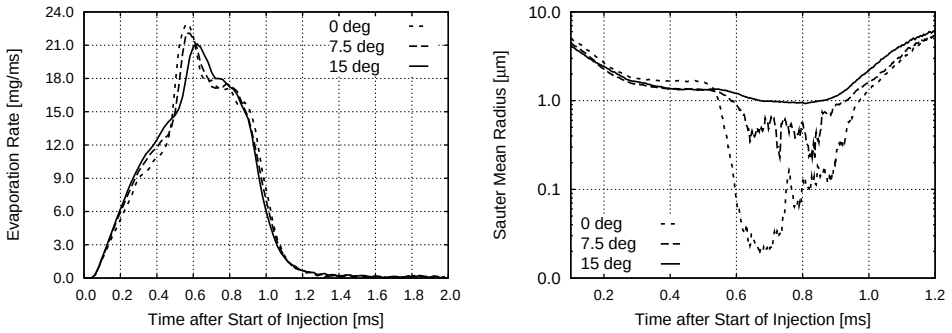


(a) Evaporation rate (b) Sauter mean radius

**Figure 9.** Comparison of evaporation rate and sauter mean radius for varying opening angle

The influence of the opening angle on spray propagation and flow field is the focus of Fig. 10. The figure shows a liquid spray (in terms of droplets) on top of velocity vectors colored with axial velocity magnitudes on a vertical plane cut through the middle of the computational mesh. Spray propagation and flow field are studied at timings of 0.4 ms, 0.6 ms and 0.8 ms after start of injection for all the three opening angles. The opening angles and the time are noted on the figure. Due to the vertical axis of symmetry, only half of the whole spray and flow field are shown in the figure. At 0.4 ms in Fig. 10(a), axial spray penetration is very similar for all the nozzles, but the radial dispersion becomes higher with the increase in the opening angle. Vortex formed due to the fuel injection are upstream of the spray tip for all the opening angles. However, radial dispersion of spray for 7.5° and 15° opening angles lead to the interaction with the vortex. This enhanced the mixing in the radial direction for both opening angles apart from the mixing in the axial direction for all the opening angles. Higher mixing of a liquid spray with the surrounding hot air signifies higher heat transfer to the liquid fuel. Therefore, higher evaporation rates are to be expected for higher opening angles around this time, as seen in Fig. 9(a).

At 0.6 ms in Fig. 10(b), the spray penetrated further in the pressurized vessel for all the opening angles. However, at this time the axial liquid penetration is clearly higher for 0° compared to the other two opening angles. This can also be seen in Fig. 5(a). The radial dispersion remained higher for higher opening angle, as it was noticed in Fig. 10(a). Interestingly, the vortex had also moved upwards towards the spray tip, enhancing mixing in the radial direction. Therefore, in 0° mixing not only improves in the axial direction, but also in the radial direction.

Figure 10(c) at 0.8 ms shows that vortex for all the opening angles had shifted upwards from the spray tip. Though their location for all the opening angles is different. Interaction of the liquid spray with the vortex can still be noticed for 15° opening angle. Thus, the cluster nozzle with this opening angle had still some enhancement in evaporation as a result of interaction with the vortex. For 0° opening angle, axial liquid penetration seems to enhancing the fuel evaporation. The spray propagation for 7.5° opening angle is in-between the 0° and 15° opening angle. Thus, the cluster nozzle with this opening angle had contribution to evaporation from mixing in the axial as well as in the radial direction.

Distribution of mean mixture fraction, $\widetilde{Z}$, at 0.6 ms is shown in Fig. 11 for all the opening angles. The higher the value of $\widetilde{Z}$ is, the richer is the fuel-air mixture. Variation in the opening angle shows a significant effect on the $\widetilde{Z}$ distribution. For 0° opening angle, richer mixtures are located at downstream of the nozzle exit, and are radially less dispersed. For 15° opening angle, overall $\widetilde{Z}$ values are smaller than for 0° opening angle, indicating leaner mixtures. But, it is spread in a larger region than in 0°. $\widetilde{Z}$ distribution for 7.5° shows characteristics of 0° and 15° opening angles, i.e. higher axial spread compared to 15° opening angle, and wider radial spread compared to 0° opening angle.

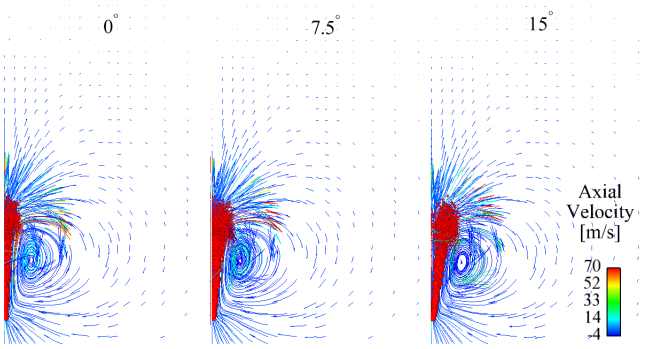


(a) 0.4 ms after start of injection

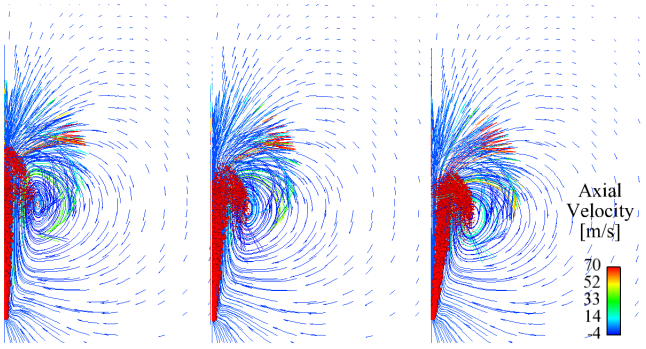


(b) 0.6 ms after start of injection

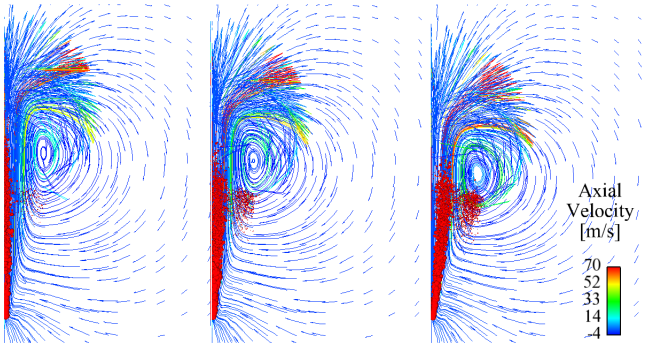


(c) 0.8 ms after start of injection

**Figure 10.** Axial velocity vectors for varying opening angle and time

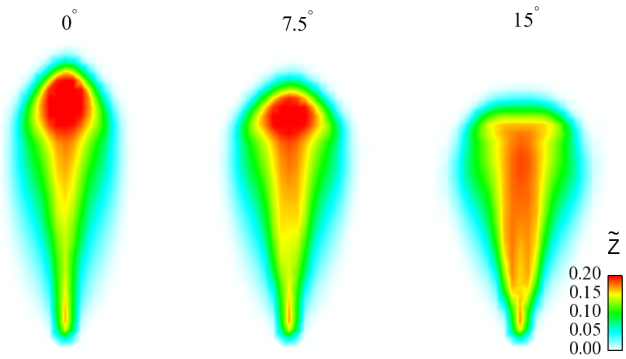


**Figure 11.** Comparison of mean mixture fraction distribution at 0.6 ms after start of injection

## Conclusions

In this study, influence of the opening angle between two sprays in diverging nozzles (cluster nozzles) was investigated through numerical simulations in a pressurized vessel at 800 K ambient temperature and 50 bar ambient pressure conditions. The opening angles, a parameter of this study, were 0°, 7.5° and 15°. The simulations were performed at evaporating conditions. The injection presssure was 1600 bar and the energizing time was 850 $\mu$s. IDEA fuel surrogate for diesel was used in the simulations. CFD code used is AC-Flux (formerly known as GMTEC).

The comparison of the computed liquid and vapor penetration lengths with the measured penetrations served as a validation of the model. Then, the computed results were analyzed to examine the influence of spray-spray interaction due to varying opening angle between the sprays on droplet breakup, spray shape and evaporation leading to mixture preparation.

In the results, the penetration length showed strong dependence on the opening angle. Liquid and vapor penetration lengths were decreased with the increase in the opening angle. Thus, nozzle with 15° opening angle had the lowest penetration (liquid and vapor), while 0° had the highest penetration. It was observed that 0° opening angle resulted in stronger spray-spray interaction compared to other two opening angles. Thereby, higher droplet collision between two sprays resulted in larger droplets causing deeper axial penetration in the vessel. While sprays from 15° opening angle appeared to be separated from each other and thus resulted in low spray-spray interaction.

For diverging nozzles, opening angle significantly affected the spray's radial distribution. Higher opening angle resulted in higher radial dispersion of liquid and vapor fuel. Variation in the radial and axial liquid fuel distribution affected spray shape. When viewed from the front, spray was mushroom shaped for 15° opening angle and spray was cone shaped for 0°. In the top view, droplets were distributed equally around the sprays, giving spherical shape for 0° opening angle. But, for higher cluster opening angle droplets were distributed more non-uniformly. The 7.5° showed intermediate results between 0° and 15°.

Liquid spray and instantaneous velocity vectors were examined to investigate the spray propagation with variation in the opening angle. Higher radial dispersion with the increase in the opening angle enhanced the interaction with the surrounding vortex (created by the sprays). For a comparable axial penetration, higher radial distribution of the sprays was advantageous for fuel evaporation with increase in the opening angle, as it was noticed till 0.5 ms after start of injection. At later times, vortices shifted downstream of the spray tip and were completely detached from the sprays. Thus in this case axial penetration of the sprays was important for the mixing of the spray with the surrounding hot air for fuel evaporation. Therefore, nozzle with lower opening angle lead to higher evaporation.

Nozzle with 7.5° opening angle had higher axial penetration than for the nozzle with 15°, and had higher radial dispersion than for the nozzle with 0°. Therefore, this nozzle combined the benefits of the nozzles with 0° and 15° opening angle.

## Acknowledgment

This work was financially supported by General Motors Corporation within the framework of the Collaborative Research Laboratory (CRL) at RWTH Aachen University.

## Nomenclature

| | |
|---|---|
| SMD | Sauter mean diameter |
| SMR | Sauter mean radius |
| CFD | Computational fluid dynamics |
| DDM | Discrete droplet model |

## References

[1] Pickett, L.M., and Siebers, D.L., *Proc. Comb. Inst.* 29:655-662 (2002).
[2] Benajes, S.B., Molina, S., De Rudder, K., Maroteaux, D., and Ben Hadj Hamouda, H., *I MECH E PART D: Journal of Automobile Engineering*, 220:1807-1817 (2006).
[3] Fasolo, B., Doisy, A., Dupont, A., and Lavoisier, F., *SAE*, 2005-01-0652, 2005.
[4] Pawlowski, A., Kneer, R., Lippert, A., and Parrish, S., *SAE*, 2008-01-0928, 2008.
[5] Gao, J., Matsumoto, Y., and Nishida K., *Atomization and Sprays*, 19(4):321-337 (2009).
[6] Nishida, K., Matsumoto, Y., and Gao, J., *Atomization and Sprays*, 19(4):339-355 (2009).
[7] Suh, H., Park, S., and Lee, C., *Proc.IMechE*, 223 (D):Journal of Automobile Engineering 1154: 1-14 (2009).
[8] Cárdenas, M., Hottenbach, P., Kneer, R., and Grünefeld, G., *SAE*, 2009-01-2771, 2009.
[9] Ewald, J., Freikamp, F., Paczko, G., Weber, J., Haworth, D. C. and Peters, N., *Technical Report*, Advance Combustion GmbH, 2003.

[10] Spiekermann, P., Jerzembeck, S., Felsch, C., Vogel, S., Gauding, M., Peters, N., *Atomization and Sprays*, 19:357-386 (2009).
[11] Barths, H., Phd thesis, RWTH Aachen University, Germany, 2001.